ISSN 1028-334X, Doklady Earth Sciences, 2022, Vol. 505, Part 1, pp. 452–458. © Pleiades Publishing, Ltd., 2022.
Russian Text © The Author(s), 2022, published in Doklady Rossiiskoi Akademii Nauk. Nauki o Zemle, 2022, Vol. 505, No. 1, pp. 53–61.

PETROLOGY

Age and Melt Sources of Ultramafic Dykes and Rocks of the Bolshetagninskii Alkaline Carbonatite Massif (Urik-Iya Graben, SW Margin of the Siberian Craton)

V. B. Savelyeva[a,*], Yu. V. Danilova[a], Academician F. A. Letnikov[a], E. I. Demonterova[a], D. S. Yudin[b], E. P. Bazarova[a], B. S. Danilov[a], and I. S. Sharygin[a]

Received January 12, 2022; revised March 25, 2022; accepted March 29, 2022

Abstract—The age of rocks of the Bolshetagninskii ijolite–syenite–carbonatite massif and ultramafic dykes within the Urik-Iya Graben in the southwestern part of the Siberian Craton was studied. An isochrone with an age of 640 ± 11 Ma was obtained by the ^{147}Sm–^{143}Nd method for rocks of the massif. $^{40}Ar/^{39}Ar$ dating of phlogopites from rocks of the dyke series provided two plateaus with ages of 644.1 ± 8.6 and 646.1 ± 8.6 Ma. The ranges of $\varepsilon_{Nd}(T)$ values corrected for 640 Ma are from +4.2 to +5.0 for rocks of the massif and from +2.9 to +4.5 for dykes and characterize a mantle source close that of OIB. Ijolite and carbonatite of the massif have $\varepsilon_{Nd}(T)$ values from +4.6 to +5.0 and $\varepsilon_{Sr}(T)$ values from –7 to –10, which indicates a common silicate–carbonate parental melt for them. Variations in the initial $(^{87}Sr/^{86}Sr)_t$ ratio from 0.7025 to 0.7059 in dykes most likely reflect both the heterogeneity in the isotopic composition of the mantle source and the different degrees of contamination of mantle melts by the material of the upper continental crust.

Keywords: allikite, picrite, ijolite, syenite, carbonatite, Sm–Nd isochrone, $^{40}Ar/^{39}Ar$ dating, Urik-Iya Graben, Siberian Craton

DOI: 10.1134/S1028334X22070169

The Urik–Iya Graben is an intracratonic structure of northwestern strike at the southwestern margin of the Siberian Craton (Fig. 1). The formation of the graben is associated with several stages of extension of the continental lithosphere in the interval of 1.91–1.53 Ga, accompanied by sedimentation and basic and granitoid magmatism [1]. Massifs of ultramafic, alkaline rocks, and carbonatite (Beloziminskii, Sredneziminskii, and Bolshetagninskii), which are associated with large reserves of Nb, Ta, U, Th, TR, P, Pb, Zn, and fluorite [3] were formed within the Urik-Iya Graben in the period between 720 and 630 Ma, during the structural transformation associated with the breakup of the supercontinent Rodinia ([2] and others). Along with alkaline rock massifs, this area is widely represented by dykes and veins of allkite, mica picrite, kimberlite-like pyroxene-free picrite, lamproite, and rare explosion pipes. However, the U–Pb and $^{40}Ar/^{39}Ar$ isotope dates have been obtained only for the Beloziminskii Massif: from 645 to 643 Ma (ID–TIMS U–Pb analysis of garnet [4] and $^{40}Ar/^{39}Ar$ dating of phlogopite [5], TIMS U–Pb analysis of zircon [2]). Isotopic dating of dyke–vein rocks was carried out mainly by the K–Ar and Rb–Sr methods. The ages obtained by the K–Ar method for picrite range from 698 to 603 Ma [6]; the $^{40}Ar/^{39}Ar$ ages of 645–622 Ma were obtained for allkitic breccia of the Beloziminskii Massif and the Yuzhnaya pipe [7]. The ages of lamproite obtained by the $^{40}Ar/^{39}Ar$, Rb–Sr, and U–Pb methods vary from 1481 to 300 Ma [8]. An isotope–geochemical study of rocks of the Bolshetagninskii Massif, which included aillikite and picrite dykes spatially associated with the massif (Fig. 1), was performed in order to detail the history of the geological evolution of the intracratonic shear zone, to clarify the sequence of the formation of mantle magmatic rocks, and to elucidate the genesis of alkaline melts.

The Bolshetagninskii Massif (Fig. 1) has a zonal ring structure due to the successive formation of ijolite–melteigite, nepheline and subalkaline syenites, and calcite and ankerite–calcite carbonatite. The massif is characterized by the wide abundance of K-feldspar syenite, which had a metasomatic effect on previously crystallized alkaline rocks [3]. Dykes of pyroxene-free phlogopite picrites intrude ijolite and syenite, but precede carbonatite or are intra-carbonatite.

[a] *Institute of the Earth's Crust, Siberian Branch, Russian Academy of Sciences, Irkutsk, 664033 Russia*
[b] *Sobolev Institute of Geology and Mineralogy, Siberian Branch, Russian Academy of Sciences, Novosibirsk, 630090 Russia*
**e-mail: vsavel@crust.irk.ru*

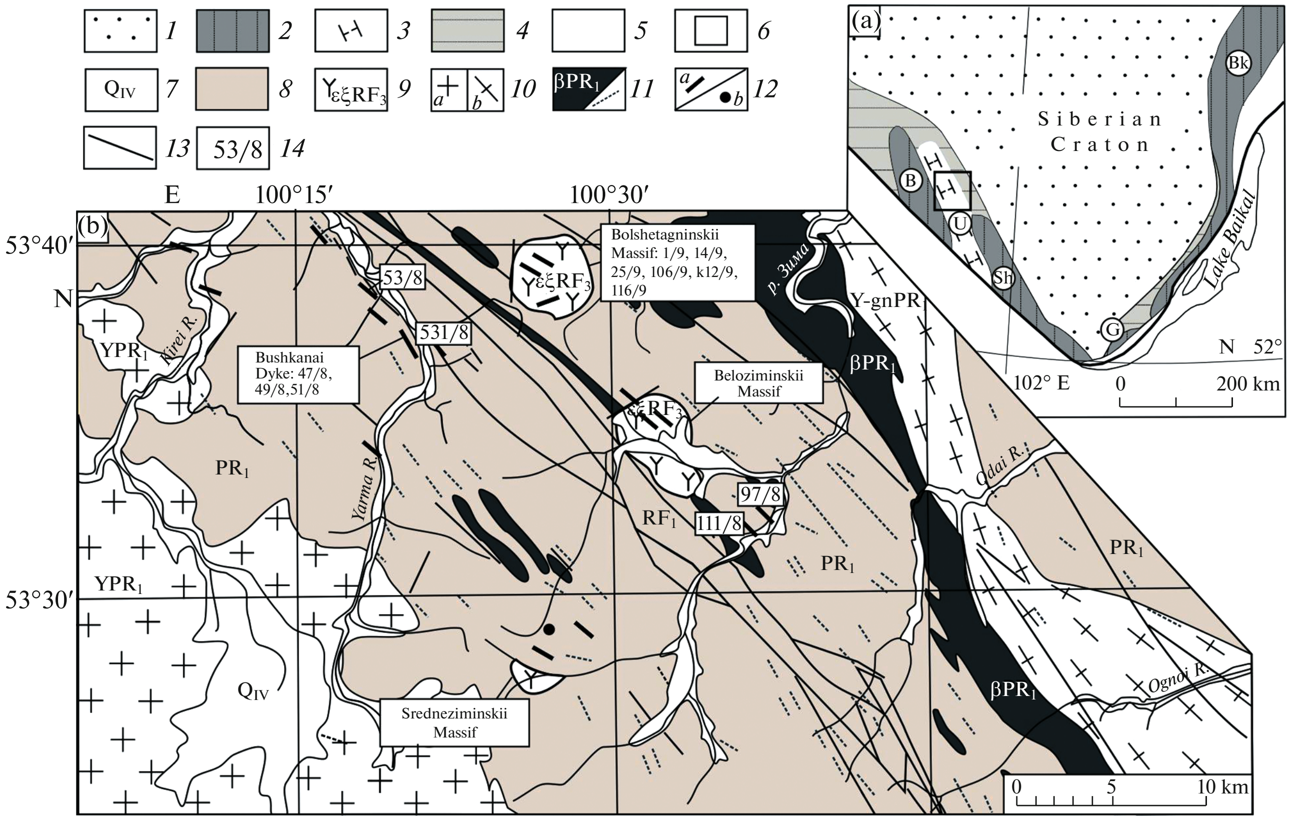

Fig. 1. Schemes of the geological structure (a) of the southern part of the Siberian Craton and (b) of the area studied. (*1*) Phanerozoic sedimentary cover; (*2*) Early Precambrian basement blocks: (Bk) Baikal, (B) Biryusinskii, (G) Goloustеn, (Sh) Sharyzhalgai; (*3*) Paleoproterozoic Urik-Iya Graben (U); (*4*) deposits of the Neoproterozoic craton margin; (*5*) Central Asian foldbelt; (*6*) location of the studied area; (*7*) Cenozoic deposits; (*8*) volcano–sedimentary deposits PR_1 and RF_1; (*9*) Ziminskii Formation of ultramafic alkaline rocks and carbonatite RF_3; (*10*) granite (*a*) and gneiss–granite (*b*) PR_1, (*11*) gabbro-diabase PR_1; (*12*) dykes, (*a*) veins and (*b*) pipes of the ultramafic composition (out of scale); (*13*) faults; (*14*) sample numbers.

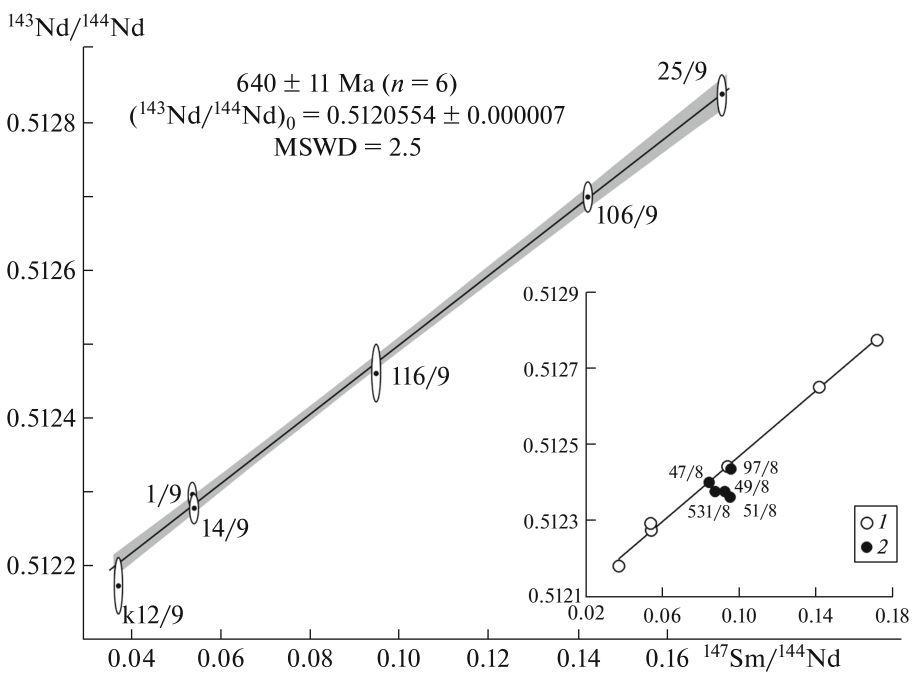

Fig. 2. Sm–Nd isochrone for rocks of the Bolshetagninskii Massif. The inset shows the position of the isotopic composition points of the dykes on the isochrones. (*1*) Rocks of the massif; (*2*) dykes of lamprophyre and picrite. Sample numbers are the same as in Table 1. The isochrone was constructed using the IsoplotR software [12].

Table 1. Sm–Nd and Rb–Sr data for rocks of the Bolshetagninskii Massif and ultramafic dykes

Sample	Rock	Sm, ppm	Nd, ppm	$^{147}Sm/^{144}Nd$	$^{143}Nd/^{144}Nd \pm 2\sigma$	$(^{143}Nd/^{144}Nd)_t$	$\varepsilon_{Nd}(T)$	Rb, ppm	Sr, ppm	$^{87}Rb/^{86}Sr$	$^{87}Sr/^{86}Sr \pm 2\sigma$	$(^{87}Sr/^{86}Sr)_t$	$\varepsilon_{Sr}(T)$
	Bolshetagninskii Massif												
25/9	Ijolite	13.07	47.04	0.1721	0.512774 ± 10	0.512053	4.7	60	1011	0.1741	0.704761 ± 16	0.703197	–8.0
106/9	Nepheline syenite	15.21	66.28	0.1421	0.512652 ± 07	0.512056	4.7	220	534	1.198	0.715105 ± 15	0.704347	8.0
K12/9	K-feldspar syenite	0.544	9.07	0.0371	0.512181 ± 12	0.512026	4.2	–	–	–	–	–	–
1/9	Calcite carbonatite	9.33	107.5	0.0537	0.512292 ± 06	0.512067	5.0	4.6	390	0.0541	0.703762 ± 14	0.703276	–7.0
14/9	Calcite–dolomite carbonatite	21.7	248.0	0.0541	0.512275 ± 07	0.512048	4.6	29.6	898	0.0930	0.703897 ± 13	0.703061	–10
116/9	Pyroxene-free phlogopite picrite (dyke)	10.62	69.50	0.0946	0.512439 ± 10	0.512390	4.5	66	72	1.425	0.715267 ± 15	0.702468	–19
	Dykes outside the massif												
97/8	Allikite	12.95	83.71	0.0958	0.512435 ± 10	0.512033	4.3	40	179	0.8589	0.711370 ± 13	0.703655	–2
531/8	Allikite	44.57	314.4	0.0878	0.512385 ± 10	0.512017	4.0	130	120	3.203	0.731732 ± 16	0.702966	–11
	Bushkanai Dyke:												
47/8	Poor-mica picrite	17.98	131.7	0.0845	0.512399 ± 14	0.512044	4.5	42.9	39	0.6577	0.711518 ± 11	0.705610	26
49/8	Mica-rich picrite	9.66	64.40	0.0929	0.512374 ± 14	0.511984	3.3	75	141	1.557	0.719438 ± 14	0.705455	24
51/8	Olivinite	3.01	19.61	0.0950	0.512360 ± 15	0.511961	2.9	9	15	1.795	0.721932 ± 13	0.705811	29

All rocks were treated with 2_HHCl prior to the isotope studies. The $^{147}Sm/^{144}Nd$ and $^{87}Rb/^{86}Sr$ values were analyzed by isotopic dilution. The analytical errors for the $^{147}Sm/^{144}Nd$ and $^{87}Rb/^{86}Sr$ ratios are 0.5 and 1.5%, respectively. The $(^{143}Nd/^{144}Nd)_t$, $\varepsilon_{Nd}(T)$, $(^{87}Sr/^{86}Sr)_t$, and $\varepsilon_{Sr}(T)$ values were calculated for an age of 640 Ma. Modern chondrite values: $^{147}Sm/^{144}Nd = 0.1967$ and $^{143}Nd/^{144}Nd = 0.512638$ [9]. The modern values of the bulk composition of the Earth are $^{87}Rb/^{86}Sr = 0.0816$ and $^{87}Sr/^{86}Sr = 0.7045$ [10]. The ^{87}Rb decay constant (1.3972) was taken from [11].

Table 2. Results of $^{40}Ar/^{39}Ar$ geochronological study of phlogopite from ultramafic dykes

T, °C	*t*, min	^{40}Ar, 10^{-9} ncm^3	$^{40}Ar/^{39}Ar$	±1σ	$^{38}Ar/^{39}Ar$	±1σ	$^{37}Ar/^{39}Ar$	±1σ	$^{36}Ar/^{39}Ar$	±1σ	Ca/K	$\Sigma^{39}Ar$ (%)	Age, Ma	±1σ
47/8 phlogopite (13.47 mg)														
J = 0.006095 ± 0.000097; total age = 645.8 ± 8.6 Ma														
500	10	1.9	16.5	0.25	0.074	0.0110	–	–	0.0009	0.0002	–	0.1	170.1	3.6
650	10	11.5	32.9	0.07	0.042	0.0014	–	–	0.0258	0.0039	–	0.5	258.1	11.6
800	10	238.7	72.1	0.03	0.017	0.0005	–	–	0.0075	0.0005	–	4.3	640.1	8.7
850	10	479.2	71.1	0.02	0.015	0.0002	–	–	0.0041	0.0005	–	11.9	640.5	8.6
900	10	810.0	71.7	0.01	0.013	0.0001	–	–	0.0034	0.0002	–	24.7	646.1	8.7
925	10	558.8	71.5	0.02	0.015	0.0002	–	–	0.0011	0.0001	–	33.5	649.9	8.7
950	10	548.4	70.9	0.02	0.014	0.0002	–	–	0.000013	0.000002	–	42.3	648.1	8.7
975	10	862.6	71.4	0.01	0.013	0.0001	–	–	0.0006	0.0002	–	55.9	650.3	8.7
1000	10	204.3	70.7	0.05	0.015	0.0005	–	–	0.0043	0.0008	–	59.2	636.4	8.7
1050	10	741.7	72.0	0.02	0.014	0.0001	–	–	0.0021	0.0002	–	70.9	651.7	8.7
1075	10	275.6	71.3	0.04	0.015	0.0002	–	–	0.0011	0.0004	–	75.2	648.6	8.7
1130	10	1572.4	71.8	0.01	0.014	0.0001	–	–	0.0024	0.0001	–	100.0	649.3	8.7
53/8 phlogopite (18.61 mg)														
J = 0.006161 ± 0.000099; total age = 648.1 ± 8.7 Ma														
500	10	2.2	4.9	0.05	0.10109	0.00302	–	–	0.0000	0.0001	–	0.3	54.0	1.0
650	10	4.5	8.3	0.06	0.08525	0.00287	–	–	0.0236	0.0062	–	0.6	14.8	20.3
800	10	1431.0	74.7	0.01	0.01538	0.00008	–	–	0.0058	0.0001	–	12.6	670.0	9.0
850	10	2237.1	72.3	0.01	0.01483	0.00003	–	–	0.0015	0.0001	–	32.0	660.8	8.9
900	10	1655.2	71.1	0.01	0.01515	0.00006	–	–	0.0010	0.0001	–	46.6	653.2	8.8
950	10	1224.4	70.1	0.02	0.01513	0.00009	–	–	0.0014	0.0001	–	57.6	644.4	8.7
1000	10	677.7	67.3	0.01	0.01873	0.00012	–	–	0.0011	0.0002	–	63.9	623.3	8.5
1050	10	593.2	67.4	0.02	0.01879	0.00017	–	–	0.0026	0.0003	–	69.4	620.8	8.5
1100	10	2535.1	70.7	0.01	0.01361	0.00002	–	–	0.0011	0.0001	–	91.8	650.2	8.8
1130	10	929.2	71.3	0.02	0.01538	0.00021	–	–	0.0021	0.0003	–	100.0	652.2	8.8
111/8 phlogopite (29.26 mg)														
J = 0.006060 ± 0.000096; total age = 641.1 ± 8.5 Ma														
650	10	2.9	28.7	0.36	0.04819	0.01268	–	–	0.0078	0.0145	–	0.1	268.3	40.7
850	10	2621.6	71.8	0.01	0.01404	0.00005	–	–	0.0037	0.0001	–	23.6	643.1	8.6
900	10	2162.7	71.6	0.01	0.01375	0.00007	–	–	0.0021	0.0001	–	43.1	645.6	8.6
950	10	2367.9	71.4	0.01	0.01384	0.00003	–	–	0.0011	0.0001	–	64.6	646.0	8.6
1000	10	1065.1	71.1	0.01	0.01427	0.00011	–	–	0.0014	0.0002	–	74.2	643.4	8.6
1050	10	1455.4	71.0	0.01	0.01406	0.00009	–	–	0.0012	0.0001	–	87.5	642.6	8.6
1100	10	302.9	67.6	0.06	0.01815	0.00036	–	–	0.0043	0.0007	–	90.4	609.3	8.4
1130	10	1026.6	68.8	0.01	0.01663	0.00009	–	–	0.0022	0.0001	–	100.0	623.7	8.4

The measurements were carried out by stepwise heating using the methodology of [13].

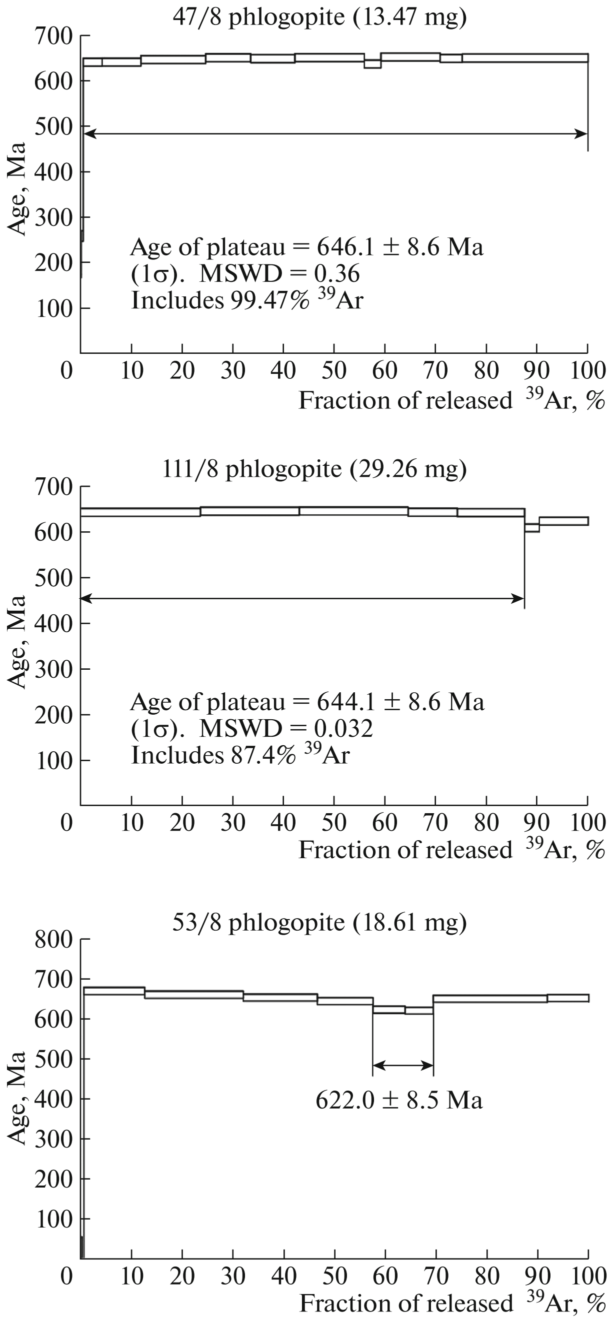

Fig. 3. $^{40}Ar/^{39}Ar$ age spectra for phlogopite from ultramafic dykes.

Ultramafic dykes intrude sand–shale deposits PR_1 and rocks of the massifs (Fig. 1b). The dykes have a steep dip, thickness from a few tens of centimeters to 10–20 m, and a length of up to hundreds of meters. Most of the dykes are represented by allkite. Among the phenocrysts in this rock are partially serpentinized olivine Fo_{82-88}, phlogopite, and titanomagnetite. The groundmass is composed of olivine, phlogopite, calcite (10–40%), diopside, titanaugite; kaersutite, aegirine, microcline, and albite are also registered. Accessory minerals are represented by chrome spinels, titanomagnetite, perovskite, manganilmenite, apatite, etc.

One of the dykes, known as the Bushkanai Dyke (Fig. 1), is petrographically heterogeneous. The dyke is composed of picrite consisting of serpentinized olivine (15–20%) and minor phlogopite in the groundmass of serpentine, diopside, hornblende, phlogopite, andradite, chrome spinels, titanomagnetite, perovskite, apatite, calcite, etc. Picrite contains melanocratic inclusions with a size up to 20 cm composed of serpentinized olivine by 80–85%; minor minerals are represented by chromium diopside, chloritized phlogopite, calcite, serpentine, chrome spinels, titanomagnetite, apatite, and andraditic garnet. In addition, veinlets with indistinct boundaries are detected in picrite. They are enriched in clinopyroxene, namely chromium diopside, augite, and titanaugite (20–25%), and mica (10–15%), but depleted in olivine (~5%).

The dykes of the Bolshetagninskii Massif are represented by phlogopite pyroxene-free picrite. Phenocrysts in this rock include serpentinized olivine and phlogopite; the groundmass consists of serpentine, serpentinized olivine, phlogopite, calcite, chlorite, melanite, grossular–andraditic garnet, monticellite, accessory chrome spinels, titanomagnetite, perovskite, apatite, Fe, Ni, and Cu sulfides, etc.

The age of the formation of the Bolshetagninskii Massif was studied by the ^{147}Sm–^{143}Nd method (Table 1). An isochrone with an age of 640 ± 11 Ma was obtained for the samples of ijolite, nepheline syenite, K-feldspar syenite, calcite, and calcite–dolomite carbonatite (Fig. 2). The points for picrite from dykes and allikite plot on or near the isochrone (Fig. 2, inset), which indicates the genetic relationship of rocks with the general event of melting of the upper mantle.

$^{40}Ar/^{39}Ar$ dating of phlogopite from allkite (Samples 53/8 and 111/8) and picrite (Sample 47/8) was performed in order to estimate the age of the dykes. The results are reported in Table 2; the age spectra are shown in Fig. 3; the measurement errors given in the text and in the figures correspond to the interval of ±1σ. To evaluate the "excess argon," the authors calculated the ages using the isochrone regression method as well. It was not possible to obtain isochrones suitable for publication; at the same time, construction of isochrones did not show the presence of "excess argon."

The $^{40}Ar/^{39}Ar$ age spectra of Samples 111/8 and 47/8 have well-defined age plateaus corresponding to 644.1 ± 8.6 Ma and 87.4% of the released ^{39}Ar and 646.1 ± 8.6 Ma and 99.4% of the released ^{39}Ar, respectively (Fig. 3). Sample 53/8 has a "saddle" shape of the age spectrum. This spectrum does not provide reliable geochronological information.

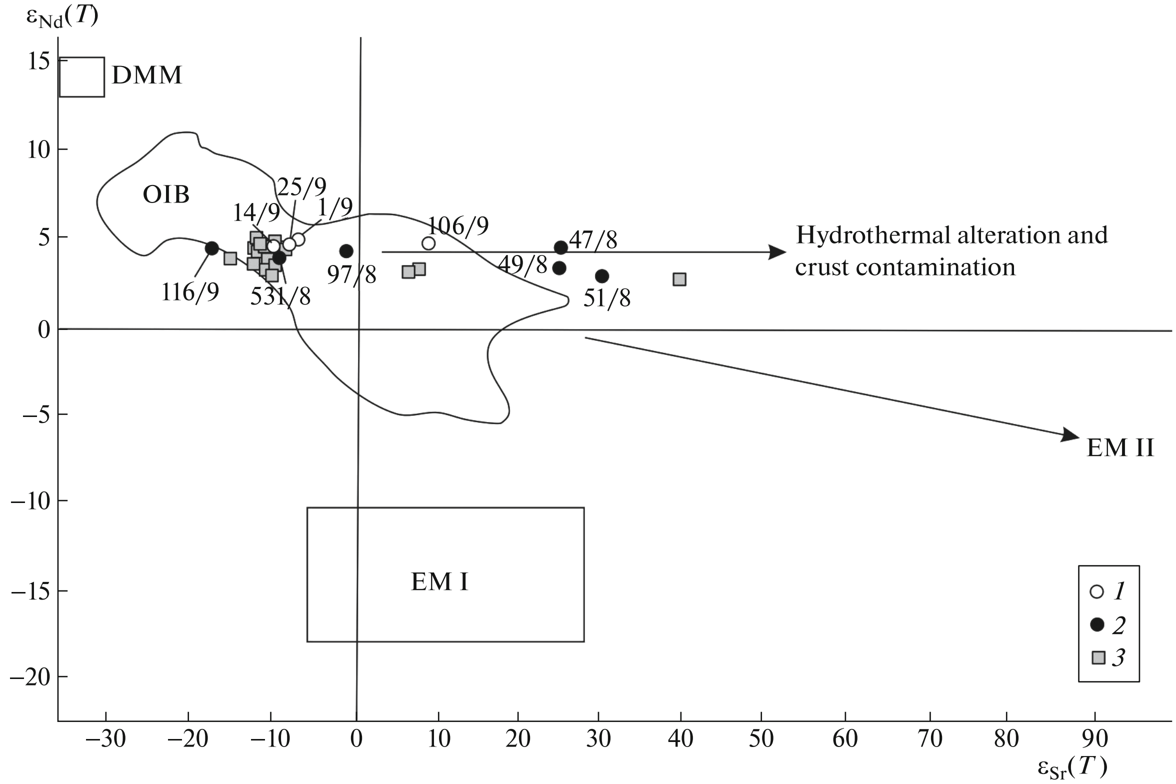

Fig. 4. Diagram $\varepsilon_{Nd}(T)$–$\varepsilon_{Sr}(T)$ for rocks of the Bolshetagninskii Massif and ultramafic dykes. (*1*) Rocks of the massif, data of the authors; (*2*) dykes of lamprophyre and picrite; (*3*) alkaline rocks and carbonatite of the Beloziminskii, Sredneziminskii, and Bolshetagninskii massifs, after [14, 15]. DMM and OIB fields and the EM I and EM II components are shown after [17].

The values of $\varepsilon_{Nd}(T)$ corrected for the age of 640 Ma range from +4.2 to +5.0 for rocks of the Bolshetagninskii Massif including the picrite dyke (Table 1). At the same time, the $(^{87}Sr/^{86}Sr)_t$ value shows the following variations: 0.7031–0.7033 in ijolite and carbonatite, 0.7044 in nepheline syenite, and 0.7025 in picrite. The values of $\varepsilon_{Nd}(T)$ and $(^{87}Sr/^{86}Sr)_t$ for allikite are close to those of ijolite and carbonatite of the massif (Table 1), while the rocks of the Bushkanai Dyke demonstrate a higher value of $(^{87}Sr/^{86}Sr)_t$ 0.7055–0.7059 and a wider range of the $\varepsilon_{Nd}(T)$ value (from +2.9 to +4.5, Table 1).

The previously obtained ages for the Beloziminskii Massif vary from 622 to 645 Ma [2, 4, 5, 7]. Our data on the age of the rocks of the Bolshetagninskii Massif, as well as allkite and picrite outside the massif, coincide with these ages within the error.

The values of $\varepsilon_{Nd}(T)$ and $\varepsilon_{Sr}(T)$ in the rocks of the Bolshetagninskii Massif and allikite correspond to the values obtained by other authors for the alkaline–carbonatite massifs of the Urik–Iya Graben [14, 15] (Fig. 4). These rocks had a single mantle source close to OIB by the isotope characteristics. The enrichment of rocks in incompatible microelements suggests that the metasomatic alteration of the mantle substrate preceded melting [16].

Ijolite and carbonatite of the Bolshetagninskii Massif have close $\varepsilon_{Nd}(T)$ and $\varepsilon_{Sr}(T)$ values (Table 1, Fig. 4) indicating separation of alkaline silicate and carbonate melts from the same parental magma. The high $(^{87}Sr/^{86}Sr)_t$ ratio in nepheline syenite (Sample 106/9) may be due to the metasomatic impact by feldspar syenite on this rock, which is expressed in microclinization accompanied by the introduction of Rb. An alternative is the contamination of the nepheline–syenite melt by the upper crustal material enriched in radiogenic Sr, but depleted in REEs.

$(^{87}Sr/^{86}Sr)_t$ variations in pyroxene-free picrite composing dykes (Sample 116/9) and allikite (Samples 531/9 and 97/8), most likely, indicate the different degrees of mantle substrate phlogopitization, which stimulates the increase in the Rb/Sr and $^{87}Sr/^{86}Sr$ ratios.

Samples 47/8, 49/8, and 51/8 from the Bushkanai Dyke occupy a separate position on the $\varepsilon_{Nd}(T)$–$\varepsilon_{Sr}(T)$ diagram (Fig. 4). The high $(^{87}Sr/^{86}Sr)_t$ value may be due to the contamination by the upper crustal material with a high $^{87}Sr/^{86}Sr$ ratio. Unfortunately, there are no data on the Sr isotope composition in the rocks of the Urik-Iya Graben. The lower $\varepsilon_{Nd}(T)$ value in olivinite (Sample 51/9) and mica picrite (Sample 49/9) compared to picrite (Sample 47/9), which composes most of the dyke (Table 1), suggests that the rocks combined in the dyke are not the products of crystallization differentiation of the same ultramafic melt, but are derivatives of different melts.

The spatial alignment and similar age of ultramafic dykes and alkaline carbonatite massifs indicate their genetic commonality, i.e., the relation of the same episode of melting of moderately depleted mantle that underwent preliminary metasomatic enrichment in incompatible trace elements. Variations in the $\varepsilon_{Sr}(T)$ value in the rocks reflect both the heterogeneity of the isotopic composition of the mantle source or, possibly, the process of contamination by the rocks of the upper continental crust, which is especially pronounced for the rocks of the Bushkanai dyke.

ACKNOWLEDGMENTS

The authors are sincerely grateful to the reviewers, whose comments contributed to a significant improvement in the quality of the manuscript.

FUNDING

This study was supported by the Russian Science Foundation, project no. 18-17-00101. The isotope analysis of Sr and Nd was performed at the Institute of the Earth's Crust, Siberian Branch, Russian Academy of Sciences (Irkutsk), using the equipment of the Center for Collective Use "Geodynamics and Geochronology," supported by grant no. 075-15-2021-682. The Ar/Ar measurements were carried out at the Center for Collective Use "Multi-element and Isotope Studies of the Siberian Branch, Russian Academy of Sciences" at the at the Institute of Geology and Mineralogy, Siberian Branch, Russian Academy of Sciences (Novosibirsk).

CONFLICT OF INTEREST

The authors declare that they have no conflicts of interest.

REFERENCES

1. D. P. Gladkochub, A. M. Mazukabzov, A. M. Stanevich, T. V. Donskaya, Z. L. Motova, and V. A. Vanin, Geotectonics **48** (5), 359–371 (2014). https://doi.org/10.1134/S0016852114050033
2. V. V. Yarmolyuk, V. I. Kovalenko, E. B. Sal'nikova, A. V. Nikiforov, A. B. Kotov, and N. V. Vladykin, Dokl. Earth Sci. **404** (7), 986–991 (2005).
3. A. A. Frolov and S. V. Belov, Geol. Ore Deposits **41** (2), 94–114 (1999).
4. E. B. Salnikova, A. R. Chakhmouradian, M. V. Stifeeva, E. P. Reguir, A. B. Kotov, Y. D. Gritsenko, and A. V. Nikiforov, Lithos **338–339**, 141–154 (2019).
5. A. G. Doroshkevich, I. V. Veksler, I. A. Izbrodin, G. S. Ripp, E. A. Khromova, V. F. Posokhov, A. V. Travin, and N. V. Vladykin, J. Asian Earth Sci. **116**, 81–96 (2016). https://doi.org/10.1016/j.jseaes.2015.11.011
6. Yu. A. Bagdasarov, S. N. Voronovskii, L. V. Ovchinnikova, and M. M. Arakelyants, Dokl. Akad. Nauk **254** (1), 171–175 (1980).
7. I. Ashchepkov, S. Zhmodik, D. Belyanin, O. N. Kiseleva, N. Medvedev, A. Travin, D. Yudin, N. S. Karmanov, and H. Downes, Minerals **10**, 404 (2020). https://doi.org/10.3390/min10050404
8. S. I. Kostrovitsky, D. A. Yakovlev, I. S. Sharygin, D. P. Gladkochub, T. V. Donskaya, I. G. Tretiakova, A. M. Dymshits, A. P. Sekerin, and V. G. Malkovets, in *Lamproites and Related Rocks: Tracers to Supercontinent Cycles and Metallogenesis,* Ed. by Krmíček L. and N. V. Chalapathi Rao (Geol. Soc. London, 2021).
9. S. B. Jacobsen and G. J. Wasserburg, Earth Planet. Sci. Lett. **67** (2), 137–150 (1984).
10. G. Faure, *Principles of Isotope Geology* (Wiley, 1986).
11. I. M. Villa, P. D. Bievre, N. E. Holden, and P. R. Renne, Geochim. Cosmochim. Acta **164**, 382–385 (2015). https://doi.org/10.1016/j.gca.2015.05.025
12. P. Vermeesch, Geosci. Front. **9**, 1479–1493 (2018).
13. A. V. Travin, D. S. Yudin, A. G. Vladimirov, S. V. Khromykh, N. I. Volkova, A. S. Mekhonoshin, and T. B. Kolotilina, Geochem. Int. **47** (11), 1107–1125 (2009).
14. N. V. Vladykin, in *Problems of Deep Magmatism Sources and Plumes* (Sochava Inst. Geogr., Siberian Branch Russ. Acad. Sci., Irkutsk, 2005), pp. 13–29 [in Russian].
15. E. A. Khromova, A. G. Doroshkevich, and I. A. Izbrodin, Geosfern. Issled., No. 1, 33–55 (2020). https://doi.org/10.17223/25421379/14/3
16. L. N. Kogarko, Y. Lahaye, and G. P. Brey, Mineral. Petrol. **98**, 197–208 (2010). https://doi.org/10.1007/s00710-009-0066-1
17. A. Zindler and S. Hart, Annu. Rev. Earth Planet Sci. **14**, 493–571 (1986). https://doi.org/10.1146/annurev.ea.14.050186.002425

Translated by A. Bobrov